Growth dynamics and morphology of passive films

I. Nainville,[1] A. Lemarchand,[2] and J.-P. Badiali[1]

[1]*Laboratoire de Structure et Réactivité aux Interfaces, CNRS URA 1662, Université Pierre et Marie Curie, 4 place Jussieu, 75252 Paris Cedex 05, France*

[2]*Laboratoire de Physique Théorique des Liquides, CNRS URA 765, Université Pierre et Marie Curie, 4 place Jussieu, 75252 Paris Cedex 05, France*

(Received 14 September 1995; revised manuscript received 6 November 1995)

We study the passive layer formation observed when a metal is immersed in an oxidizing solvent and propose a model based on two different schemes to describe the evolution of the solid film and the liquid phase. The formation of the passive layer is simulated at a mesoscopic scale, whereas the concentrations in soluble species in the liquid are deduced from the numerical resolution of a macroscopic equation. The evolution of the two phases is coupled by the particular boundary conditions imposed at the moving interface. The simulation model involves reaction and diffusion processes, including a poisoning of the traveling interface due to chemical species initially added to the solvent or produced by the growth reaction itself. Depending on the parameter values, in particular on the production of poison during the growth reaction, different asymptotic behaviors are reached. The simulation brings out the existence of a large parameter domain in which the system spontaneously evolves toward a critical state. This behavior follows a short transient regime associated with the growth of a thin compact structure. The existence of such a primary layer in contact with the metal has been invoked in the literature to explain experimental results on lithium batteries. In stationary conditions, the layer observed is porous and characterized by a self-similar geometry. We find an order parameter whose fluctuations are controlled by the diffusion coefficient of the poisoning species and have a power-law behavior. The concept of self-organized criticality has been proposed to unify such a dynamical regulation around a critical state in an open nonlinear spatiotemporal system. We believe that the growth of thick films offers an example of this behavior.

PACS number(s): 68.45.−v, 82.20.Wt, 82.20.Mj, 64.60.Ak

I. INTRODUCTION

The growth dynamics of thick films and the mechanisms governing the selection of their morphology have not yet been totally elucidated. Among these complex spatiotemporal processes, the passivation of a metal is a subject of substantial fundamental and practical interest [1–19].

In this paper, we study the passive layer formation observed when a metal is immersed in an oxidizing solvent. This phenomenon has received particular attention owing to its industrial implications in the optimization of lithium battery performances [1–18]. During the storage of a liquid cathode battery before its use, the lithium anode is covered by a thick insulating layer. This passive layer will disturb the current passage when the battery will be used as a generator [1–3]. Nevertheless, the use of a liquid cathode confers specific properties on the cell, which justifies its preferential choice in many military and civil applications in spite of the nuisance to the anode.

The passive layer formed on the anode has been observed by means of scanning electron microscopy and may reach a width of 100 μm [2]. A class of existing macroscopic models has been elaborated upon from a comparison with experimental impedance measurements. They usually assume that the passive film is constituted by two sublayers, a thin compact primary sublayer and a thick porous secondary sublayer [4–9]. It is to be noted that the compact primary layer has never been directly detected but its suspected existence and its properties are supposed to determine the amplitude of the instantaneous voltage drops observed during the first discharge of the battery [1–3,10]. The characteristics of the voltage recovery that follows are imputed to the morphology of the secondary porous layer. Many experimental studies have been devoted to the variables that may affect the voltage delay effect. These variables include the nature and the concentration of species present in the solvent. In particular, some of these additives induce morphological modifications revealed by alleviation of the voltage delay effect [2,3,10–14]. The role played by the sulfur dioxide, which can be added to the liquid phase, is specific since it is also produced by the growth reaction itself. Note that the composition of the layer is not affected by the use of additives [2,15].

Our goal, in this paper, is to build a simulation model, based on physical hypotheses, which attempts to capture the main features of the passivation process. Our aim is not to come to a quantitative comparison with experimental results but to bring out the minimal ingredients necessary to understand the early growth of thick films. We assume that the layer growth is controlled by reaction-diffusion processes. We draw particular attention to the chemical reactions occurring at the interface between the passive layer and the solvent. It is essential to describe the possible adsorption of some chemical species on the reactive sites of the interface. As a conse-

quence, the description of the diffusion of these blocking additives in the liquid phase will also be crucial to discuss the further growth or the poisoning of the reactive interface.

The paper is organized as follows. Bringing out first the elementary processes governing the beginning of the passivation, we then detail in Sec. II the simulation procedure. Section III is devoted to the simulation results obtained for a constant or a spatiotemporal description of the blocking probability deduced from the additive concentration. In this last case, we propose to interpret the regulation of porous growth around a critical state in terms of self-organized criticality. In particular, we determine the scaling laws that characterize the layer morphology, such as fractal properties. We conclude in Sec. IV.

II. THE SIMULATION MODEL

Our study is applied to the lithium anode passivation by a lithium chloride layer during the storage of a lithium–thionyle chloride cell. Note that we do not analyze the effects of current passage.

A. The elementary processes governing the beginning of the passivation

The passivation of a planar surface of lithium immersed in thionyle chloride, $SOCl_2$, involves a large number of elementary chemical reactions. Nevertheless, a reduced kinetic model is commonly admitted [16–18]. The first step consists in the oxidation of the lithium metal according to

$$\mathrm{Li} \rightarrow \mathrm{Li}^+ + e^- \ . \tag{1}$$

In the second step, the thionyle chloride is reduced at the solid-liquid interface and the lithium chloride precipitates on the previously formed layer according to

$$4\mathrm{Li}^+ + 4e^- + 2\mathrm{SOCl}_2 \rightarrow 4\mathrm{LiCl} + \mathrm{SO}_2 + \mathrm{S} \ , \tag{2}$$

where the produced sulfur dioxide, SO_2, is soluble in the solvent. Reaction (2) takes place in the presence of some soluble additives A and salts like $LiAsF_6$.

Experiments [2,3,10–14] have shown that the presence of additives A in the solvent as well as the concentration of SO_2 itself play a major role in the LiCl layer structure. In order to account for the influence of additives including SO_2, we make the following conjecture: the layer growth may be locally hindered by blocking effects induced by the presence of additives A on the layer-solvent interface. According to this hypothesis, reaction (2) is likely to occur only in so-called reactive interfacial sites, denoted R, in opposition to blocked interfacial sites, denoted B. The blocking phenomenon may be modeled by the following nonreversible step:

$$R + A \rightarrow B \ . \tag{3}$$

We admit that the role played by additives, including SO_2, in the interface poisoning is the same whatever their chemical nature. Figure 1 gives a schematic representation of the phenomena leading to the formation of the

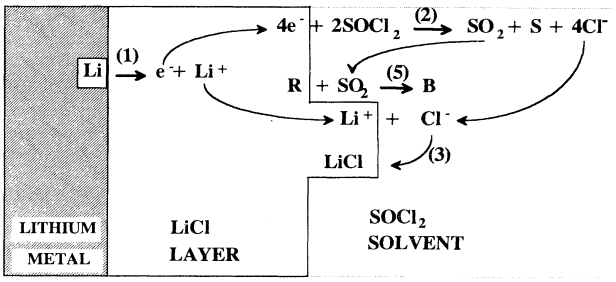

FIG. 1. Schematic representation of the reaction-diffusion processes governing the LiCl passive layer growth.

LiCl layer. It exhibits two boundaries moving in two opposite directions: a solid-solid interface between the lithium metal and the LiCl layer and a solid-liquid interface between the LiCl layer and the solvent. Reaction (1) occurs at the solid-solid interface whereas reaction (2) takes place at the solid-liquid interface. Consequently, the further LiCl layer growth requires the transport of Li^+ ions and electrons through the previously formed layer from the Li-LiCl interface up to the LiCl-solvent interface [20]. We wish to model the very beginning of the passive layer growth. At this early stage of LiCl formation, the passive layer is very thin and we assume that the limiting step with respect to Li^+ diffusion is the lithium corrosion step given by Eq. (1). In this model, we neglect the backward movement of the Li-LiCl interface due to the metal corrosion and assume that this interface remains straight. We thus admit that a constant number of Li^+ ions reaches the layer-solvent interface maintaining it out of equilibrium. We wish to examine the possibility of a structure change from a compact to a porous growth. At this early stage, the diffusion of $SOCl_2$ may be neglected and the liquid phase may be considered as a reservoir of $SOCl_2$ [21].

To sum up, we choose to model the passivation of the metal by reaction and diffusion processes. The kinetic model reduces to three elementary steps labeled (1), (2), and (3). We think that it is crucial to follow the evolution of blocking species concentration in the neighborhood of the reactive interface, which requires the description of their diffusion in the liquid phase.

B. The simulation procedure

The LiCl layer growth appears as a complex spatiotemporal out-of-equilibrium phenomenon. In order to investigate the heterogeneous processes governing the layer growth, we propose a simulation scheme that combines two distinct methods and proposes descriptions of the solid and liquid phases at two different levels. An analogous approach has also been adopted to study solidification under nonequilibrium conditions [22,23]. In our case, the solid phase growth simulates a generalized percolation cluster growth at a mesoscopic scale. In a pure percolation cluster growth model, an interfacial solvent site R is transformed with a probability p into a blocked site B or into a new solid site with a probability

$1-p$. The specificity of our simulation growth model is to introduce a blocking probability $p(x,y,t)$ that depends on both space (x,y) and time t, proportionally to the concentration in blocking agents $A(x,y,t)$. Thus, the blocking probability is a dynamical variable governed by the diffusion of additives in the liquid phase. The evolution of the additive concentration, $A(x,y,t)$, in the liquid phase is not simulated but deduced from the numerical resolution of a deterministic diffusion equation with particular boundary conditions imposed by the growing solid front.

Contrary to the solid phase evolution that includes fluctuation effects, the liquid phase evolution is described at a macroscopic level. The two different schemes adopted to describe the solid and the liquid phases are intimately intricate since the local growth of the solid depends on the blocking probability or equivalently on the concentration in additives in the site considered. Reciprocally, the evolution of the additive concentration depends on the boundary conditions imposed by the moving interface itself.

At the mesoscopic level chosen to simulate the solid phase, we consider a square lattice of constant a in which each site represents a group of molecules of a given species. It can be occupied by solid species, Li and LiCl, or by a solvent species. We define a reactive site R as an interfacial solvent site that has at least a side in common with a LiCl site. A reactive site R may be transformed into a blocked site B through reaction (3). Thus, a site may be occupied by five different species. A solid site occupied by the lithium metal or by LiCl is respectively labeled M or L. A liquid site may be labeled R, B, or S if it is respectively a reactive, blocked, or noninterfacial solvent site. Double occupancy of a lattice site is forbidden. This coarse graining allows us to study the phenomena occurring at a length scale greater than the lattice constant a. For computing-time requirements, we simulate a two-dimensional (2D) medium.

Initially, the interface between the metal and the solvent is a straight line in the direction y at which the reactions (1), (2), and (3) occur, corroding the metal and covering it by a layer of LiCl. Neglecting the metal corrosion, the Li-LiCl interface remains a straight line. The growing interface between LiCl and the solvent propagates in the direction x perpendicularly to the initial metal surface. Periodic boundary conditions are imposed in the direction y.

As mentioned above, we assume a constant corrosion rate; i.e., we assume that, due to reaction (1), a constant number Φ of Li^+ ions is formed during one time unit. This hypothesis leads to a constant time interval Δt between two successive creations of a LiCl site. We recall that a site contains a large number of molecules. Taking into account the size and structure differences between the primitive cells of LiCl and Li crystals, the corrosion of a lithium site leads to the formation of α LiCl sites with $\alpha > 1$. The time interval Δt between two successive creations of a LiCl site is chosen as the simulation time unit and may be expressed in terms of physical constants by

$$\Delta t = 1/\alpha\Phi \ . \tag{4}$$

We introduce discrete space and time variables as

$$i = \frac{x}{a}, \quad j = \frac{y}{a}, \quad s = \frac{t}{\Delta t} \ , \tag{5}$$

where i, j, and s are integers, a is the lattice constant, and Δt is the time unit.

In the simulation procedure, the concentration in additives in each solvent site has to be calculated. The same cell size a is chosen to describe the solid and liquid phases. The additive concentration is supposed to be constant in a cell but varies due to diffusion from one cell to another. The initial concentration in additives A_0 is homogeneous and eventually equal to zero. The same blocking probability p_0 is initially assigned to each interfacial site according to

$$p_0 = k A_0 \ , \tag{6}$$

where k is the normalization constant.

Whatever time s, the blocking probability at the interfacial solvent site of coordinates (i,j) is given by

$$p_{i,j,s} = k A_{i,j,s} \ , \tag{7}$$

where $A_{i,j,s}$ is the concentration of additives in this site.

A simulation step consists in a growth step leading to the formation of a new LiCl site and in an update of the additive concentration in the solvent. The processes of growth and diffusion are executed sequentially.

During a growth step occurring at time s, a first reactive site R of coordinates (i_0,j_0) is randomly chosen and irreversibly transformed into a blocked site B with an instantaneous local blocking probability $p_{i_0,j_0,s}$ or into a LiCl site L with a probability $1-p_{i_0,j_0,s}$. The additive concentration in this site is updated, whatever its new nature, B or L, according to

$$A_{i_0,j_0,s'} = 0, \quad \forall s' > s \ . \tag{8}$$

Actually, the solvent has been either pushed by the formation of a new LiCl solid site L or irreversibly trapped in a blocked site B, which is no longer concerned with diffusion processes. If the site (i_0,j_0) has been transformed into a site L, its nearest neighbors, which are occupied by a solvent species, become reactive sites R and the growth step ends. Otherwise, a new reactive site R is chosen and this procedure is repeated until a reactive site is actually transformed into a LiCl site L. Note that it may occur after several transformations of reactive sites R into blocked sites B.

The growth step is followed by an updating of the additive concentrations in each solvent site of nature R or S. The transformation of a reactive site at (i_0,j_0) into a site L locally increases the concentration in additives and introduces source terms in the equation governing the evolution of the additive concentration in the nearest-neighbor solvent sites. More precisely, the particular boundary conditions imposed by the growing LiCl front lead to the following discrete equation for the additive concentrations in a solvent site R or S located at (i,j):

$$A_{i,j,s+1}=A_{i,j,s}+d\,(A_{i+1,j,s}+A_{i-1,j,s}+A_{i,j+1,s}+A_{i,j-1,s}-\beta_{i,j,s}A_{i,j,s})$$
$$+(\delta_{i,i_0+1}\delta_{j,j_0}+\delta_{i,i_0-1}\delta_{j,j_0}+\delta_{i,i_0}\delta_{j,j_0-1}+\delta_{i,i_0}\delta_{j,j_0+1})\left[\frac{q}{\beta_{i_0,j_0,s}}+\frac{A_{i_0,j_0,s}}{\beta_{i_0,j_0,s}}\right], \quad (9)$$

where the parameter d is given by

$$d=D\Delta t/a^2, \quad (10)$$

$\beta_{i,j,s}$ is the number of nearest neighbors of cell (i,j) occupied by a solvent species R or S at time s. Note that the additive concentration in a site (i,j) of species M, L, or B at time s obeys $A_{i,j,s}=0$. The quantity q, homogeneous to a concentration, is deduced from the amount of SO_2 formed by the chemical reaction (2) during Δt in the cell (i_0,j_0). The last term in Eq. (9) represents the concentration increase due to the growth reaction (2) and to the progression of the solid phase in the site (i_0,j_0), which has pushed forward the liquid. This local excess has been shared among the nearest neighbors of site (i_0,j_0). Note that the same time unit Δt defined in Eq. (4) is chosen to simulate the solid phase and to integrate the diffusion equation (9) in the liquid phase. Then a new cycle of growth and diffusion is executed, and so on.

The simulation model reduces to the classical Eden model [24–26] for a vanishing blocking probability $p=0$. It presents analogies with the percolation cluster growth model [26,27] if p remains homogeneous in space and stationary in time.

III. RESULTS

A. Constant and homogeneous poisoning

Before examining the results deduced from the simulation model presented in Sec. II B, we first give the main properties of the structures obtained for a stationary and homogeneous blocking probability p. In the frame of this simple model, the LiCl layer growth crucially depends on the value of the single parameter p. We observe a bifurcation between a growth regime and a totally poisoned regime for a critical value p_c of the blocking probability p. This critical value is related to the percolation threshold p_p of the blocked sites. The value of p_c depends on the dimension of the lattice and equals

$$p_c=0.405\pm0.005\approx 1-p_p \quad (11)$$

for a square lattice of dimension 2 [26,28].

Figure 2 represents the bifurcation diagram obtained.

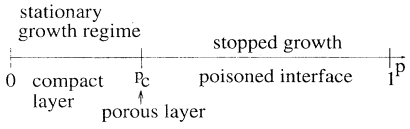

FIG. 2. Bifurcation diagram in the case of a stationary and homogeneous blocking probability p. Stability domains of the asymptotic regimes observed for different values of p.

In a large parameter domain, the model accounts for the stationary growth of a rather compact and homogeneous structure as shown in Fig. 3(a). A porous structure given in Fig. 3(b) develops only in critical conditions.

More quantitatively, the different growth regimes may be characterized by the time evolution of the number n_R of reactive sites R, as seen in Fig. 4. If $p<p_c$, the number of reactive sites, n_R, slightly fluctuates around a stationary value. On the contrary, one observes for $p\approx p_c$ large fluctuations around a smaller mean stationary value. This amplification of the fluctuations near p_c characterizes the vicinity of the transition. If $p>p_c$, the number of

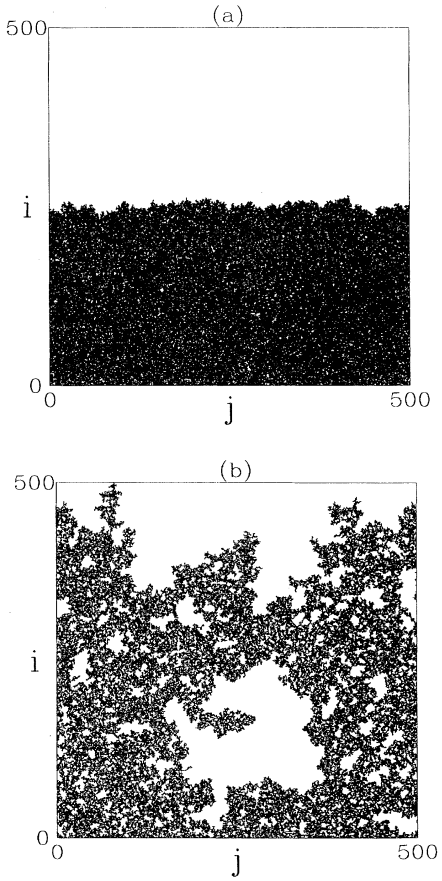

FIG. 3. Snapshots of the LiCl passive layer simulated on a 500×500 lattice with a stationary and homogeneous blocking probability p. The front propagates in the direction x labeled i. The lithium metal is represented by the straight line $i=0$. LiCl sites are black, solvent sites are white. (a) For $p=0.2$, compact stationary growth in noncritical conditions, (b) for $p=0.405$, porous stationary growth in critical conditions.

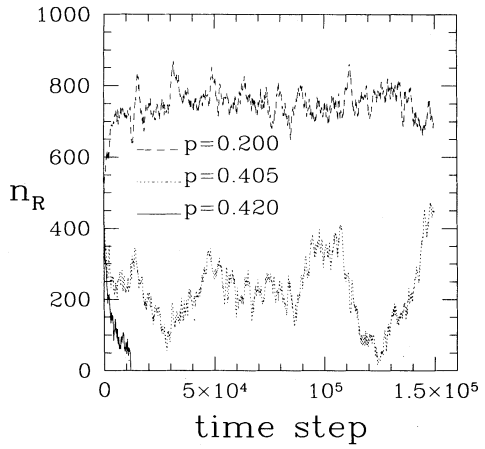

FIG. 4. Time evolution of the number n_R of reactive sites for different values of the stationary and homogeneous blocking probability p.

reactive sites decreases and finally vanishes when the interface is totally poisoned.

The two different growth regimes observed for $p<p_c$ and $p=p_c$ may also be characterized by the fractal properties of the simulated layer. From a computational point of view, the most efficient method to determine the fractal dimension is the box-counting method [26,29]. The layer structure appears as a cloud of points embedded in a 2D space. Covering the 2D space by a grid and defining $N(r)$ as the number of square boxes of side r necessary to cover the layer, we plot $\log_{10}[N(r)]$ versus

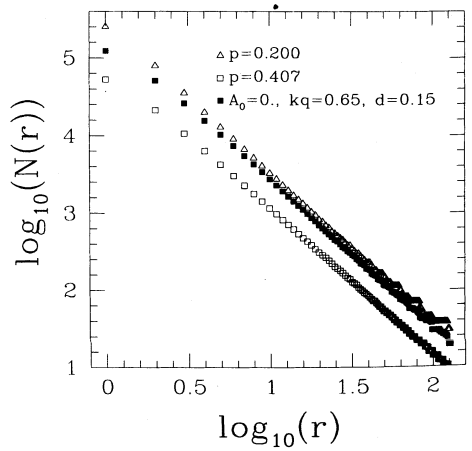

FIG. 5. The box-counting method: determination of the covering dimension or capacity D_0^S of LiCl layers simulated from two different models. $N(r)$ is the number of square boxes of side r necessary to cover the interface. The open symbols correspond to simulation results on a 1500×1500 lattice for a stationary and homogeneous blocking probability p. The curves drawn with open triangles (△) and open squares (□) are respectively obtained in noncritical ($p=0.200$) and critical ($p=0.405$) conditions. The solid squares (■) correspond to simulation results on a 500×500 lattice for a dynamically controlled blocking probability $p(x,y,t)$ in the parameter domain II where the dynamics maintains the system in critical conditions.

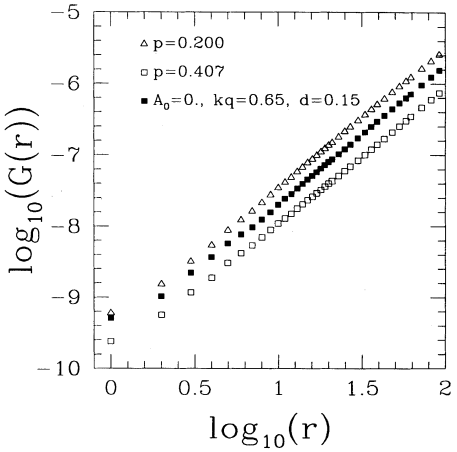

FIG. 6. The Grassberger-Procaccia method: determination of the correlation dimension D_2^S of LiCl layers simulated from two different models. $G(r)$ is the spatially averaged number of layer sites in a disc of radius r. The meanings of the symbols are identical to those in Fig. 5.

$\log_{10}(r)$. The modulus of the slope of the linear region characterizes the global fractal properties of the structure. It is known as the covering dimension or capacity D_0^S. Results are given in Fig. 5. In the region where $p<p_c$, we find

$$D_0^S(p<p_c)=1.98\pm0.02\ , \tag{12}$$

whereas we obtain in critical conditions

$$D_0^S(p=p_c)=1.88\pm0.02\ . \tag{13}$$

The Grassberger-Procaccia method [26,29,30] gives access to another fractal dimension, the correlation dimension D_2^S. Defining $G(r)$ as the spatially averaged number of layer sites in a disk of radius r, we plot $\log_{10}[G(r)]$ versus $\log_{10}(r)$. The slope of the linear region is the correlation dimension. Results are given in Fig. 6 and lead to

$$\begin{aligned} D_2^S(p<p_c)&=1.98\pm0.02\ , \\ D_2^S(p=p_c)&=1.87\pm0.02\ . \end{aligned} \tag{14}$$

The values of the fractal dimensions deduced from the box-counting method and from the Grassberger-Procaccia method are in very good agreement, proving that the structures are not multifractal [29]. Moreover, the values of D_0^S and D_2^S are close to the theoretical predictions in the case of the percolation cluster growth model. In particular, the structures that develop in the domain where $p<p_c$, associated with a dimension very close to 2 cannot be considered as fractal. On the contrary, the layer that exists for $p=p_c$ is qualitatively different, and possesses a self-similar structure characterized by a fractal dimension smaller than 2. We find with a good precision the value $\frac{91}{48}$ predicted in the frame of the percolation cluster growth model [26,31].

The fractal properties of the instantaneous interface between the previously formed LiCl layer and the liquid phase may also be used to discriminate between the two

different kinds of structures. In order to determine the interface, it is essential to define two dual sets of sites [32,33]. The metal is supposed to be at the bottom of the system and the solvent at the top. We give the label 1 to solid sites M and L. Liquid sites R, B, and S are labeled 0. The interface is defined as the last line of nodes labeled 1, which are connected to the bottom boundary through first neighbors and which are first or second neighbors to nodes labeled 0, which are themselves connected to the top boundary by the same rule, i.e., through first or second neighbors [32,33]. The instantaneous lattice state can be viewed as a coast with an earth possessing lakes and a sea. Note that there are no islands since the reactive sites are defined as first neighbors to previously formed sites in order to ensure the mechanical rigidity of the layer.

To determine the front of solid species or interface, we use an algorithm proposed by Hoshen and Kopelman in the frame of the percolation theory [27,34]. The correlation dimension D_2^I of the interface is determined in Fig. 7 from the Grassberger and Procaccia method. In noncritical conditions, the interface width is small and the front appears as a straight line at large scale. Consequently, the slope of the curve associated with $p<p_c$ in Fig. 7 tends to 1 as soon as the disk radius around an interfacial site exceeds 10 lattice sites. The determination of the fractal dimension is only possible in a narrow interval of small disk radii and is not accurate. We find

$$D_2^I(p<p_c)=1.45\pm0.05 \ . \tag{15}$$

Within the uncertainties, we recover the theoretical value 1.50 predicted for an interface obtained from the Eden model [26]. In critical conditions, the interface is large and ramified. It is quantitatively characterized by the following fractal dimension:

$$D_2^I(p=p_c)=1.58\pm0.02 \ . \tag{16}$$

The value we obtain seems larger than the value 1.5 associated with the Eden model. As mentioned by Gouyet [26], the fractal dimension of the interface differs from the value 1.75 associated with an infinite percolation cluster [26,31,32,35,36].

To sum up, let us point out that, for a constant and homogeneous poisoning, the porous growth appears only in marginally stable conditions at the frontier between a compact growth regime and a totally poisoned regime where growth is stopped. This result, which restricts the porous growth to a very particular parameter value, does not agree with the observation of porous structures whatever the experimental conditions. In order to describe the existence of a compact layer close to the metal followed by a thick porous layer, a model that includes a temporal evolution of the growth conditions is required. In particular, it is necessary to follow the dynamics governing the concentration in blocking species.

B. Dynamically controlled poisoning

In this section, we give the simulation results obtained when the blocking probability $p(x,y,t)$ is deduced from the dynamical evolution of the additive concentration in the liquid phase according to Eq. (9). In order to differentiate the effect of the four parameters A_0, k, q, and d on the growth dynamics, we first consider two limit cases corresponding either to an absence of initial supply in additives or to a negligible production of SO_2 by chemical reaction (2).

Imposing first a vanishing initial concentration in additives, $A_0=0$, only two parameters are independent. The bifurcation diagram obtained is given in Fig. 8 in the parameter space (d,kq). The influence of d on the layer structure type is not very great and the relevant parameter is the product kq. Note that, due to the finite difference scheme used to solve Eq. (9), the value of d obeys $d<0.25$ [37].

The value p_c still corresponds to a critical limit between two different regimes. Whatever the diffusion coefficient value d, a stationary compact growth regime is reached when the parameter kq is smaller than the critical probability p_c. Figure 9(a) gives a snapshot of the layer obtained in these conditions. In this parameter

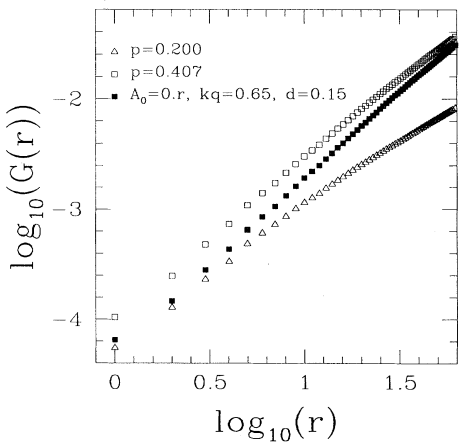

FIG. 7. Determination of the correlation dimension D_2^I of the layer interfaces using the Grassberger-Procaccia method. The meanings of the symbols are identical to those in Fig. 5.

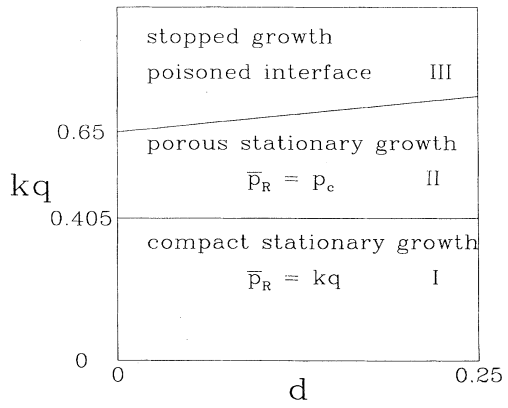

FIG. 8. Bifurcation diagram in the case of a dynamically controlled blocking probability $p(x,y,t)$ in the absence of initial supply in additives ($A_0=0$).

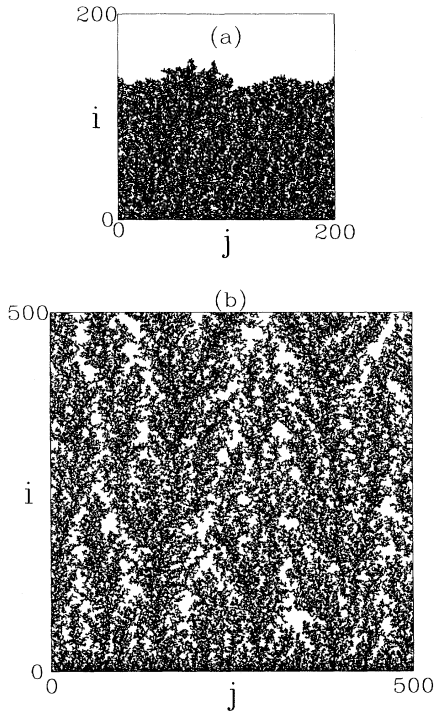

FIG. 9. Snapshots of the LiCl passive layer for a dynamically controlled blocking probability $p(x,y,t)$ in the absence of initial supply in additives ($A_0=0$) and for the following parameter values: (a) simulation on a 200×200 lattice in domain I, $kq=0.2$, $d=0.15$, after a transient regime, a compact growth regime is stabilized; (b) simulation on a 500×500 lattice in domain II, $kq=0.65$, $d=0.15$, after a transient regime, a porous growth regime is stabilized.

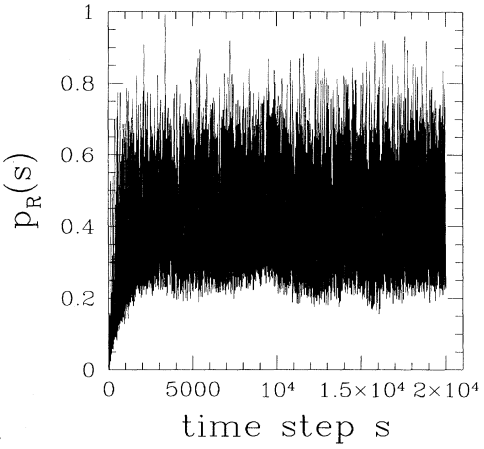

FIG. 10. Mean blocking probability value $p_R(s)$ in the interfacial sites randomly chosen between s and $s+1$ and transformed into blocked sites or into a new LiCl site versus time step s. The parameter values are the same as in Fig. 9(b).

domain, labeled I, the situation is quite similar to the case of a constant probability described in Sec. III A. The layer cannot be considered as fractal but appears as a compact structure of dimension 2. We define the mean probability $p_R(s)$ in the interfacial sites R, which react between time steps s and $s+1$, i.e., which are transformed either into blocked sites or into a new LiCl site during this time unit Δt. The increase of $p_R(s)$ at small time proves the existence of a transient regime. Then, one observes the stabilization of $p_R(s)$ around at time-averaged value $\bar{p}_R$ equal to

$$\bar{p}_R = kq \quad \text{for } 0<kq<p_c, \quad \forall d \ . \tag{17}$$

It is noteworthy that the mean stationary value $\bar{p}_R$ is independent of the diffusion coefficient d and is entirely fixed by kq, i.e., by the SO_2 quantity liberated by chemical reaction (2).

When kq crosses the critical limit p_c, a poisoning of the interface is not observed but a porous growth is stabilized in a large parameter domain labeled II. As shown in Fig. 8, this parameter domain is bounded from below by the line $kq=p_c$, whatever d and from above by a line that is not parallel to the d axis. Actually, for a fixed value of kq, the poisoning of the interface is intuitively easier for small d since the additives remain a longer time in the vicinity of the interface. Figure 9(b) gives a snapshot of the porous layer obtained in these conditions. The time evolution of $p_R(s)$ is given in Fig. 10. We first observe a transient regime during which the blocking probability goes from 0 to a fluctuating stationary value. The evolution at short time, characterized with a low but increasing interface poisoning, is associated with the formation of a thin compact layer that becomes more and more porous with time. In this parameter domain, our simulation model gives account for the existence of a thin compact layer, formed during the transient regime and followed by a different structure developing in stationary conditions. The striking result is that the blocking probability of reactive sites is dynamically driven toward the critical value p_c. Whatever the parameter values inside domain II, the time-averaged value of the blocking probability of reactive sites is locked at the marginally stable value p_c. When the stationary regime is reached, we have

$$\bar{p}_R = p_c \tag{18}$$

in the parameter domain labeled II in Fig. 8.

Qualitatively, the fluctuations of the blocking probability $p_R(s)$ in reactive interfacial sites vary with the value of the diffusion coefficient d. The amplitude of these fluctuations may be measured by the ratio of the standard deviation and the mean value, $\sqrt{\langle (p_R-\bar{p}_R)^2\rangle}/\bar{p}_R$, or equivalently [32,35,38–43] by the quantity $\langle |p_R-\bar{p}_R|\rangle/\bar{p}_R$, where $\langle\ \rangle$ stands for a time average. As shown in Fig. 11, the fluctuations fit the following power law over more than a decade:

$$\frac{\langle |p_R-\bar{p}_R|\rangle}{\bar{p}_R} \propto d^{-\eta} \ , \tag{19}$$

where the exposant η is equal to

$$\eta = 0.17 \pm 0.02 \ . \tag{20}$$

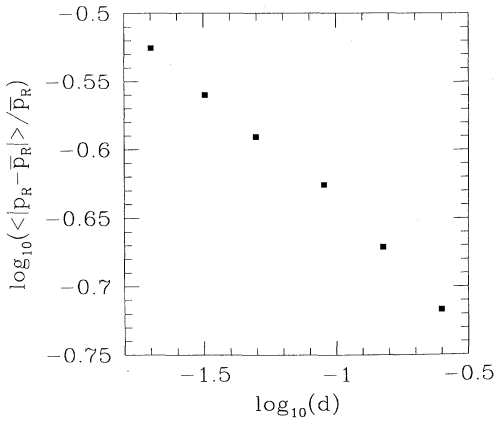

FIG. 11. Scaling law verified by the fluctuations of the blocking probability $p_R(s)$ in interfacial sites. Log_{10}-$\log_{10}$ plot of the ratio $\langle|p_R-\bar{p}_R|\rangle/\bar{p}_R$ vs adimensional diffusion coefficient d, where $\langle\ \rangle$ stands for a time average.

In domain II, the layer structure appears porous and the analysis of its fractal properties, using the box-counting method and the Grassberger-Procaccia method leads respectively to

$$D_0^S(\text{domain II})=1.87\pm0.02\ ,$$
$$D_2^S(\text{domain II})=1.88\pm0.02\ , \tag{21}$$

as given in Figs. 5 and 6. These values are very close to the fractal dimensions given in Eqs. (13) and (14) in the case of critical homogeneous and stationary blocking probability p_c. They agree with the theoretical prediction equal to $\frac{91}{48}$ in the frame of the percolation cluster growth model [26,31].

The interface between the solid LiCl layer and the liquid phase given in Fig. 12 possesses also a self-similar structure of fractal dimension

$$D_2^I(\text{domain II})=1.60\pm0.02\ , \tag{22}$$

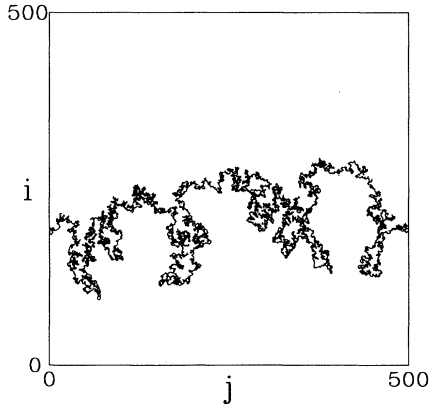

FIG. 12. Instantaneous external boundary of the LiCl layer obtained for a dynamically controlled blocking probability for $A_0=0$, $kq=0.65$, and $d=0.15$.

determined from the Grassberger-Procaccia method in Fig. 7. This value agrees with the fractal dimension found in the case of a critical homogeneous and stationary blocking probability and given in Eq. (16).

Finally, the bifurcation diagram given in Fig. 8 exhibits a third parameter domain labeled III. In this domain, the growth is irreversibly stopped due to the interface poisoning.

We consider now the limit case where the amount of SO_2 produced by chemical reaction (2) is negligible with respect to the initial supply in additives. In this case, the parameter q tends to 0 and the relevant variable is the product kA_0. The bifurcation diagram obtained in the parameter space (d,kA_0) is given in Fig. 13. It is noteworthy that domain II, which corresponds in Fig. 8 to a porous growth, is now restricted to the line $\gamma kA_0=p_c$, where the coefficient γ is approximately equal to 2.

In the general case where we consider the effect of initial supply in additives ($A_0\neq0$) as well as the production of SO_2 during the growth ($q\neq0$), the obtainment of a bifurcation diagram is more tricky. The influence of d on the layer structure remains weak, the relevant parameter is now $k(q+\gamma A_0)$ where the coefficient γ is still equal to 2. The bifurcation diagram in the parameter space $(d,k(q+\gamma A_0))$ crucially depends on A_0. Roughly speaking, there still exist three domains such as those in Fig. 8 for a vanishing A_0 but the size of domain II in which a critical growth is stabilized reduces as A_0 increases.

These simulation results exhibit the specific role played by the sulfur dioxide, SO_2, in the existence of a large parameter domain associated with a porous growth. It seems essential that poisoning species are produced locally directly in the neighborhood of interfacial sites to ensure the development of a porous structure. It is then necessary that the simulation model carefully describes the dynamical evolution of the concentration in SO_2 in order to account for the regulation of the layer growth. Qualitatively, we interpret the stabilization of a porous growth in the following way: a strong local growth of the

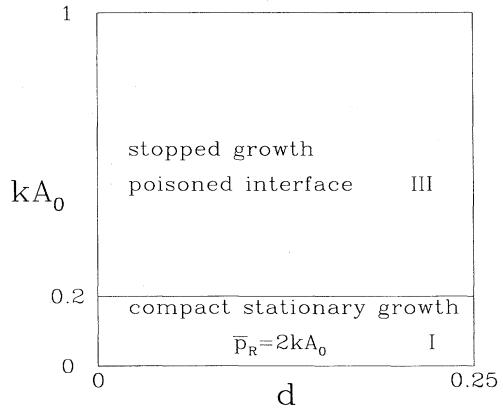

FIG. 13. Bifurcation diagram in the case of a dynamically controlled blocking probability $p(x,y,t)$ for a negligible production of SO_2 ($q=0$).

layer releases an important amount of blocking species in the neighborhood but it leads to the formation of a solid finger pointing toward the solvent. Thus, the evacuation of the poison through diffusion is much easier than in the case of a plane interface. In other words, the ramification of the solid structure increases the contact with the liquid phase and facilitates the poison dispersion, which will enable a new growth process. We think that this feedback mechanism ensures a stabilization of the marginally stable state associated with the critical value of the blocking probability.

We wish to bring out the differences between our model and the self-organized depinning model [44–47] (SOD) introduced to describe wetting phenomena. In this last case, the properties of the interface are governed by the evolution of the height $h(y)$ of each liquid column according to an equation of Kardar-Parisi-Zhang [48] type. In this approach, Gaussian white noises are used to reproduce the properties of the random solid medium in which the liquid front propagates. Local reorganization rules are imposed to ensure the existence of "avalanches." The critical conditions associated with SOD correspond to the directed percolation threshold and not to the 2D percolation threshold as in our case. We observe a self-organization into a critical state through the simulation of an actual 2D dynamics based on three elementary reaction or diffusion processes without introducing specific rules or stochasticity through external Langevin noises.

IV. CONCLUSION

The model we propose to mimic the passivation process of a metal [1–18] is based on two different schemes respectively associated with the description of the solid and the liquid phases [22,23]. The formation of the solid layer is simulated at a mesoscopic level that contains the description of the interfacial fluctuations that are generated by the underlying microscopic dynamics. The concentrations of soluble species in the liquid phase are deduced using a macroscopic approach. Nevertheless, the particular boundary conditions at the moving interface couple the evolution of the two phases. The simulation model allows us to study the growth dynamics as well as the morphology of the resulting layer. We show that a model that aims at the description of a morphology change with the distance from the metal necessarily includes the spatiotemporal description of the concentration in poisoning species.

Depending on the parameter values, in particular on the production of poison during the growth reaction, different asymptotic behaviors are reached. The interface may be either totally poisoned or maintained in a state associated with a permanent growth regime. Before stationary growth conditions are reached, a short transient regime is observed during which a thin compact structure develops in contact with the metal. This result provides confirmation of the existence of a primary layer that has been invoked to explain some experimental data [4–9].

The simulation brings out the existence of a large parameter domain for which the system spontaneously evolves toward the critical state. By way of contrast, we should note, in the case of a constant blocking probability, that the system evolves to a critical state only for a single value of the parameter. When the spatiotemporal description of the blocking probability evolution is introduced, the same asymptotic growth regime is reached over a wide range of parameter values leading to the formation of a porous layer. The dynamics maintains the system in marginally stable conditions very close to a total poisoning, which is never reached. It is necessary to invoke a feedback mechanism in order to give account for the regulation of the porous growth. The concept of self-organized criticality [38–43] has been proposed to unify such types of behaviors in open nonlinear spatiotemporal systems. In the case we consider, it can be viewed as a morphology-selection mechanism since it promotes a porous growth.

The system restricted to the liquid phase possesses the basic properties required to observe a natural evolution toward a critical state. Actually, the liquid phase is an open heterogeneous medium with many spatial degrees of freedom interacting through diffusion. The couplings of the liquid phase with the exterior, here the growing layer, introduce spatiotemporal and nonlinear interactions. The concentration of poisoning species near the interface or, equivalently, the blocking probability of reactive sites appears as an order parameter. Its flux, induced by the heterogeneous boundary conditions, is nonuniform in space as required in the general mechanisms leading to self-organized criticality [42,43].

Another way of characterizing this phenomenon is to point out that the system that operates in the vicinity of a critical point has no inherent length scale. The spatial structure of the layer has self-similarity over an extended range of length scales. We determine the fractal dimension [29] of the inner layer structure and the properties of its interface in contact with the solvent. We find with a good precision the fractal dimension values predicted in the frame of the classical percolation cluster growth model [26,27]. We also show that the fluctuations of the order parameter, the blocking probability associated with reactive sites, p_R, follows a power law. The fluctuations of p_R behave as $d^{-\eta}$ where the control parameter d is the diffusion coefficient of blocking species.

These different results prove without ambiguity that the few elementary reaction and diffusion processes on which the simulation model is based are sufficiently complex to generate a spontaneous evolution toward a critical state. We believe that self-organized criticality is a key mechanism in understanding a class of passivation processes occurring in the presence of poisoning agents.

[1] A. N. Dey, Electrochim. Acta **21**, 377 (1976).
[2] A. N. Dey, Thin Solid Films **43**, 131 (1977).
[3] P. Chenebault, D. Vallin, J. Thevenin, and R. Wiart, J. Appl. Electrochem. **19**, 413 (1989).
[4] E. Peled and H. Yamin, Israel. J. Chem. **18**, 131 (1979).
[5] R. V. Moshtev, Y. Geronov, and B. Puresheva, J. Electrochem. Soc. **128**, 1851 (1981).
[6] E. Peled, J. Power Sources **9**, 253 (1983).
[7] E. Peled, in *Lithium Batteries,* edited by J. P. Gabano (Academic, New York, 1983).
[8] V. E. Kazarinov and V. S. Bagomzky, J. Power Sources **20**, 259 (1987).
[9] Y. Zhang and C.-S. Cha, Electrochim. Acta **37**, 1211 (1992).
[10] W. Bowden, J. S. Miller, D. Cubbison, and A. N. Dey, J. Electrochem. Soc. **131**, 1768 (1984).
[11] A. N. Dey and J. Miller, J. Electrochem. Soc. **126**, 1445 (1979).
[12] C. R. Schlaikjer, in *Lithium Batteries* (Ref. [7]).
[13] J. W. Boyd, J. Electrochem. Soc. **134**, 18 (1987).
[14] P. Chenebault, D. Vallin, J. Thevenin, and R. Wiart, J. Appl. Electrochem. **18**, 625 (1988).
[15] D. Chua, W. Merz, and W. Bishop (unpublished).
[16] T. I. Evans and R. E. White, J. Electrochem. Soc. **136**, 2798 (1989).
[17] T. I. Evans, T. V. Nguyen, and R. E. White, J. Electrochem. Soc. **134**, 328 (1989).
[18] G. Eichinger, J. Power Sources **43**, 259 (1993).
[19] J. R. Driscoll, G. L. Holleck, and D. E. Toland (unpublished).
[20] F. M. Delnick, J. Power Sources **26**, 129 (1989).
[21] I. Nainville, A. Lemarchand, and J.-P. Badiali (unpublished).
[22] O. Shochet, K. Kassner, E. Ben-Jacob, S. G. Lipson, and H. Müller-Krumbhaar, Physica **181A**, 136 (1992).
[23] T. Ihle and H. Müller-Krumbhaar, Phys. Rev. E **49**, 2972 (1994).
[24] H. J. Herrmann, Phys. Rep. **136**, 154 (1986).
[25] J. Kertesz and D. E. Wolf, J. Phys. A **21**, 747 (1988).
[26] J.-F. Gouyet, *Physique et Structures Fractales* (Masson, Paris, 1992).
[27] A. Bunde and S. Havlin, in *Fractals and Disordered Systems,* edited by A. Bunde and S. Havlin (Springer, Berlin, 1991), p. 51.
[28] D. Stauffer, *Introduction to Percolation Theory* (Taylor & Francis, London, 1985).
[29] K. R. Sreenivasan, Annu. Rev. Fluid Mech. **23**, 539 (1991).
[30] P. Grassberger and I. Procaccia, Phys. Rev. Lett. **50**, 347 (1983).
[31] A. Bunde and J.-F. Gouyet, J. Phys. A **18**, L285 (1985).
[32] B. Sapoval, M. Rosso, J.-F. Gouyet, and J.-F. Colonna, Solid State Ionics **18-19**, 21 (1986).
[33] M. Rosso, J.-F. Gouyet, and B. Sapoval, Phys. Rev. Lett. **57**, 3195 (1986).
[34] J. Hoshen and R. Kopelman, Phys. Rev. B **14**, 3428 (1976).
[35] J.-F. Gouyet, M. Rosso, and B. Sapoval, Phys. Rev. B **37**, 1832 (1988).
[36] M. Rosso, J. Phys. A **22**, L131 (1989).
[37] J. Crank, *The Mathematics of Diffusion* (Clarendon, Oxford, 1975).
[38] P. Bak, C. Tang, and K. Wiesenfeld, Phys. Rev. Lett. **59**, 381 (1987).
[39] P. Bak, C. Tang, and K. Wiesenfeld, Phys. Rev. A **38**, 364 (1988).
[40] C. Tang and P. Bak, J. Stat. Phys. **51**, 797 (1988).
[41] B. Drossel and F. Schwabl, Phys. Rev. Lett. **69**, 1629 (1992).
[42] D. Sornette, J. Phys. (France) I **11**, 2065 (1992).
[43] N. Fraysse, A. Sornette, and D. Sornette, J. Phys. I (France) **6**, 1377 (1993).
[44] S. V. Buldyrev, A.-L. Barabási, F. Caserta, S. Havlin, H. E. Stanley, and T. Vicsek, Phys. Rev. A **45**, R8313 (1992).
[45] K. Sneppen, Phys. Rev. Lett. **69**, 3539 (1992).
[46] T. Halpin-Healy and Y. C. Zhang, Phys. Rep. **254**, 215 (1995).
[47] A.-L. Barabási and H. E. Stanley, *Fractal Concepts in Surface Growth* (Cambridge University Press, Cambridge, 1995).
[48] M. Kardar, G. Parisi, and Y. C. Zhang, Phys. Rev. Lett. **56**, 889 (1986).